Polymer Crystallization Induced by Sorption of CO_2 Gas

J. S. CHIOU, J. W. BARLOW, and D. R. PAUL, *Department of Chemical Engineering and Center for Polymer Research, University of Texas at Austin, Austin, Texas 78712*

Synopsis

Previous work has shown that sorption of CO_2 at relatively high pressures by glassy polymers reduces their glass transition temperatures and may convert the glass into a rubber under certain conditions. It is shown here that this plasticization by a gas can induce crystallization just as sorption of vapors or liquids is known to do. This point is extensively explored for miscible blends of poly(vinylidene fluoride) and poly(methyl methacrylate) and to a lesser extent for poly(ethylene terephthalate). In some cases, this secondary crystallization process results in small crystals whose melting endotherms are just above the glass transition and are very similar to peaks resulting from heat capacity overshoots, or enthalpic relaxation, caused by sub-T_g annealing; however, by appropriate techniques peaks arising from these two separate mechanisms can be distinguished. For oriented materials, evidence is shown which demonstrates that the additional crystals formed on CO_2 sorption have the same preferential orientation as the original material.

INTRODUCTION

Polymers which can crystallize are seldom in thermodynamic equilibrium; hence, their state can be altered by a variety of treatments. For example, exposure to liquid or vapor environments causes crystallization to occur in some polymers. During the past two decades the liquid or vapor induced crystallization of poly(ethylene terephthalate)[1-4] and polycarbonate[5-7] have been studied extensively. The course of the induced crystallization includes the processes of sorption and diffusion of the diluent into the polymer leading to plasticization which increases the rate of polymeric segmental motions such that rearrangement into crystals is kinetically possible. The same processes are also involved in gas–polymer systems.[8-11] To our knowledge, the possibility of crystallization induced by gas sorption has not been reported previously. However, as we have pointed out in a study of the CO_2 plasticization of polymers, the needed conditions can indeed be achieved by CO_2 gas sorption.[10] This interesting finding has an important bearing on two aspects. First, it provides another approach to create crystallinity in a polymer. While the diffusion rates and the extent of sorption in polymers for liquids and vapors are limited by their saturation state, the amount of sorption of a gas in a polymer can be continuously increased by elevating its pressure. Also the diffusion coefficient for a gas in a polymer is often increased by elevating the pressure.[11] This suggests that the rate and extent of crystallization caused by exposure to a gas such as CO_2 can be controlled by adjusting its pressure. Second, this observation implies that caution must be exercised when interpreting gas sorption and

Journal of Applied Polymer Science, Vol. 30, 3911–3924 (1985)
 CCC 0021-8995/85/093911-14$04.00

transport information for polymer systems capable of crystallization since exposure to the gas may change the state of crystallinity. Our observations arose in this context, and Figure 1 shows a good illustration of the changes which can occur for the case of miscible blends of poly(vinylidene fluoride) (PVF_2) and poly(methyl methacrylate) (PMMA). The lower curve shows the PVF_2 heat of fusion in the blend before CO_2 exposure while the upper curve shows this quantity for each sample after its CO_2 sorption isotherm had been measured. Clearly, there is higher crystallinity of PVF_2 afterwards except for blends rich in PMMA, where no PVF_2 crystallization occurred at all.

The purpose of what follows is to demonstrate that the differences noted in Figure 1 are, in fact, the consequence of crystallization induced by CO_2 sorption and to explore some of the details of the process for the various miscible blends formed from PVF_2 and PMMA. To establish generality, limited results for poly(ethylene terephthalate) are also presented.

EXPERIMENTAL

PVF_2 from Pennwalt, Kynar 460N, and PMMA from Rohm and Haas, Plexiglas V(811), were received in pellet form. Films of various blend compositions were prepared by extrusion as described elsewhere.[11,12] The extruded films had been stored at ambient conditions for about 2.5 years before they were examined by differential scanning calorimetry (DSC). Unless specified, the *quenched* PVF_2/PMMA films were prepared by heating extruded films to 170–200°C and immediately quenching them into ice water (quenching rate $\simeq$ 10⁴°C/min). This procedure eliminates the molecular orientation and any sub-T_g annealing effects from the extruded film. The poly(ethylene terephthalate) used in this study was prepared by laminating several layers of commercial 2-mil Kinmar films to achieve a final thickness of about 20 mils by heating in a press to 300°C and then quenching in ice water to give a sample of low crystallinity.

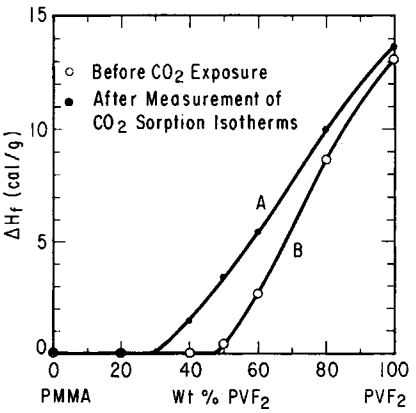

Fig. 1. PVF_2 heat of fusion for extruded PVF_2/PMMA blends: (A) after CO_2 sorption isotherm measurement; (B) prior to CO_2 exposure (samples had been at ambient temperature for a long time prior to DSC scan).

The sorption experiments were carried out by placing the sample in a stainless steel sorption cell immersed in a water bath at 35°C. Samples were exposed to the gas at a single pressure except for one set of blends which were exposed to numerous cycles of CO_2 pressure ranging from 0 to 25 atm while measuring the sorption isotherms.[11,12] Unless specified, samples were thoroughly degassed before they were examined by DSC.

The glass transition temperature, the melting point and the heat of melting or crystallization were measured by a Perkin-Elmer DSC-2 differential scanning calorimeter equipped with a Thermal Analysis Data System. In measuring the endothermic or exothermic peak areas, the baseline was subtracted using a built-in Scanning Autozero (SAZ) program. The heating rate was 20°C/min and the onset temperature was taken as the T_g. All DSC plots were normalized to unit sample mass to facilitate comparison.

The molecular orientation of the film was characterized by use of a Gaertner L305 Birefringence Measurement System employing a white light source.

RESULTS AND DISCUSSION

Miscible blends of PVF_2 and PMMA[13] can be expected to show a wide spectrum of phenomena at 25–35°C since the T_g of the former is well below this range while the T_g of the latter is well above this range. Since miscible blends have single T_g's intermediate between those of the constituents and dependent on composition, some blends will have their T_g's in this range.[13] Furthermore, one component, PVF_2, can crystallize while the other, PMMA, cannot. A variety of equilibrium and kinetic effects on crystallization behavior caused by blending have been described.[13–15]

The detailed results described here center around an additional endothermic peak for PVF_2, other than the normal melting peak, which is observed after certain thermal or gas exposure histories. The location of this peak may be anywhere from just above the T_g of the sample up to the normal melting point of PVF_2. When near the T_g, this peak resembles the heat capacity overshoot associated with sub-T_g annealing and care must be used in distinguishing the two since glassy state relaxation processes also occur in the range of 25–35°C for some of these blends as seen later.

From the above discussion, it is clear that a diverse array of events can occur for PVF_2/PMMA blends especially in the presence of a plasticizing diluent such as CO_2. A cursory overview is provided by the thermograms for various blend compositions displayed in Figures 2–4. The results in Figure 2 correspond to first heats of materials stored at ambient conditions for a long time. Figure 3 shows first heats for corresponding samples after exposure to CO_2 at pressures up to 25 atm encountered during measuring their CO_2 sorption isotherms. The results in Figure 1 correspond to the total endotherm areas in Figures 2 and 3. Figure 4 shows thermograms obtained on a second heating in the DSC after the first, and these results are independent of all prior histories of the samples. The peaks occurring over the 60–90°C range in Figures 2 and 3 but not seen in Figure 4 are the focus of our interest. Discussion of these details is most conveniently accomplished by considering each composition separately.

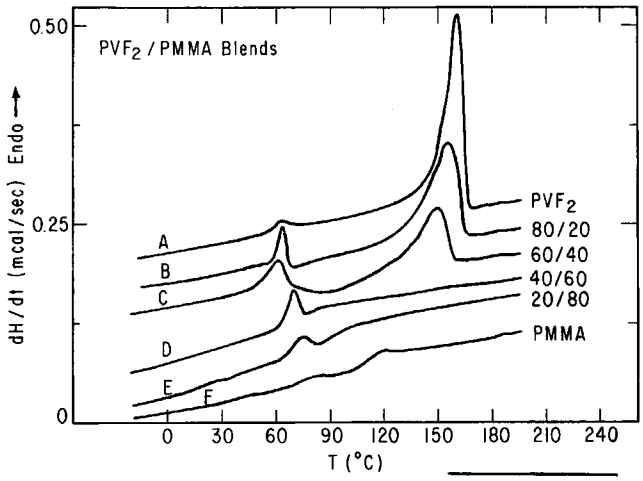

Fig. 2. Thermograms for first DSC heats of blends held at ambient temperature for a long time. Basis for curve B in Figure 1.

Poly(vinylidene Fluoride)

It is pertinent to note, from the outset, that PVF_2 exhibits an unusually broad melting endotherm. Melting begins well below the peak or apex temperature to form a highly skewed or asymmetric endotherm which is, no doubt, a result of a broad crystal size distribution. As noted in Figures 2(A) and 3(A), a small endotherm secondary to the main melting peak appears for pure PVF_2 with these histories. The secondary peak is no longer evident on a second heat, Figure 4(A), where the polymer is first melted then quenched to $-60°C$, which is below T_g[16] for this polymer, and then heated in the DSC from this state. This secondary peak is believed to represent the melting of rather small crystallites formed during ambient storage of PVF_2. Annealing PVF_2 at higher temperatures causes this peak to

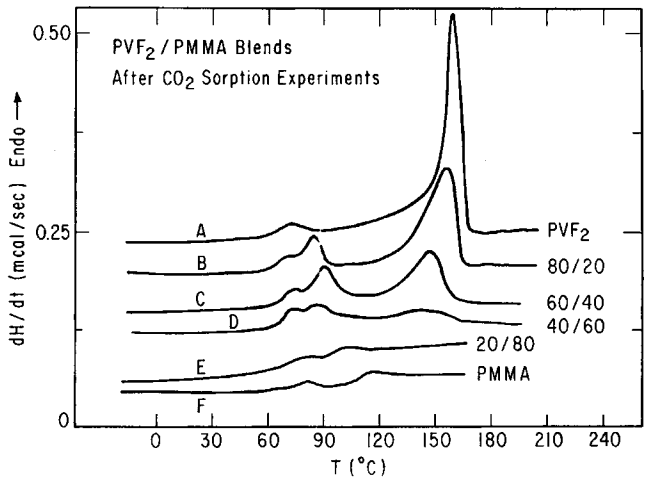

Fig. 3. Thermograms for first DSC heats of blends after CO_2 sorption isotherm measurements. Basis for curve A in Figure 1.

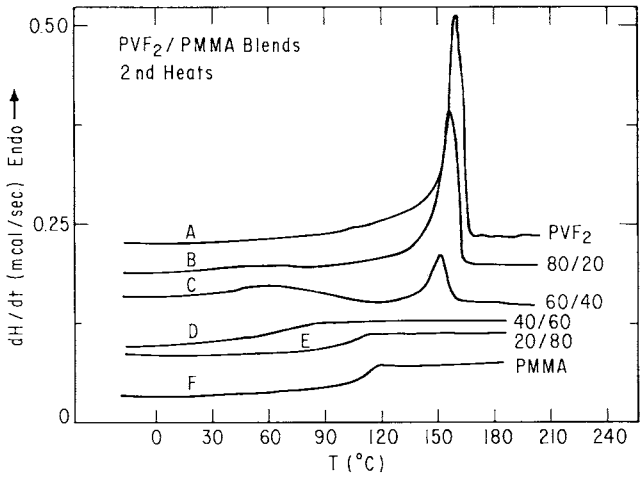

Fig. 4. Thermograms for second DSC heats of blends.

shift up the temperature scale—indicative of larger crystallites. For example, annealing at 156°C for 20 h causes the secondary peak to become superimposed on the shoulder of the primary peak and to have an apex temperature of 165°C.[15] Exposure to CO_2 causes only a minor change in this secondary peak for pure PVF_2, viz., the apex temperature increases from 64 to 72°C while the peak area increases from 0.43 to 0.56 cal/g. There are two reasons for this. First, PVF_2 has a low T_g and any plasticizing effect from CO_2 does not add much at 25–35°C to the already high mobility of these chain segments. Second, PVF_2 crystallizes rather rapidly and most cooling histories lead to high initial crystallinities, ~55%, leaving little material to participate in secondary processes. As seen next, blending with glassy PMMA dramatically alters these circumstances such that this secondary peak is greatly affected by CO_2 exposure and it becomes a useful parameter for following the changes which occur.

80% PVF_2 Blend

The as-extruded 80% PVF_2 blend has a much larger secondary peak than does PVF_2 (see Figs. 2 and 3), probably because it originally did not crystallize as much as PVF_2 and, thus, the blend has a stronger potential to crystallize subsequently under appropriate conditions. This can be understood by comparing the thermograms for these two materials in Figures 2–5. Neither sample shows any secondary peaks on the second heat in the DSC (Fig. 4). While the quenched PVF_2 has a heat of melting, ΔH_m, of 13.2 cal/g, the blend has a value of 8.5 cal/g, which is less than 80% of the former. The T_g of this blend is not discernable in Figures 2–4; however, it can just be detected by using the maximum DSC sensitivity in the low temperature region of Figure 4(B) (see inset of Fig. 5) and is found to be near room temperature. When this polymer is heated to 200°C and immediately quenched into ice water, it exhibits a very weak secondary peak followed by a significant crystallization peak in the DSC scan [Fig. 5(A)]. Holding this sample at ambient conditions permits it to slightly crystallize

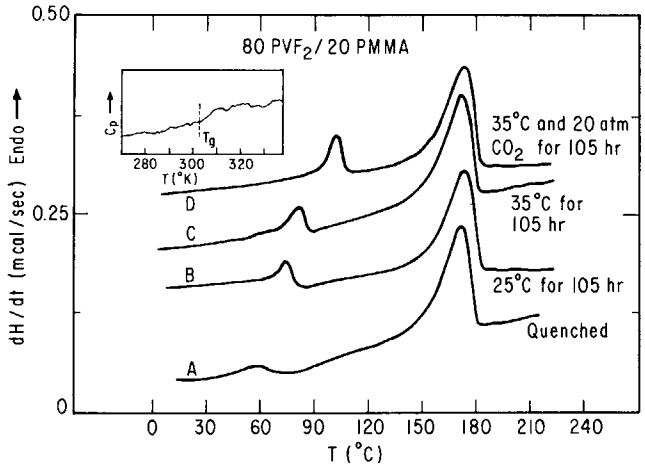

Fig. 5. First heat thermograms for 80% PVF_2 blends: (A) after quenching from the melt into ice water; (B) after holding at 25°C for 105 h; (C) after holding at 35°C for 105 h; (D) after exposure to CO_2 at 20 atm for 105 h at 35°C. The inset shows a portion of Figure 4(B) at a very high sensitivity.

further by a purely thermal effect hence the larger secondary peak [Fig. 5(B)]. Elevating the temperature to 35°C enhances the thermal effect, thus shifting the secondary peak to a higher temperature [Fig. 5(C)]. Exposing the sample at 35°C to a CO_2 environment has an even greater effect on subsequent crystallization [Fig. 5(D)]. This indicates that the polymeric molecular motions are facilitated by CO_2 sorption. The shoulder on the secondary peak in Figure 3(B), which does not show up in Figures 2(B) and 5, is believed to occur as a result of the CO_2 pressure cycling during sorption isotherm measurement.

60% and 50% PVF_2 Blends

As seen in Figure 2(C), the first heat of a 60% PVF_2 blend displays an even larger secondary peak than seen for the two previous materials. However, this peak is primarily the result of enthalpic relaxation which occurs during sub-T_g annealing[17-19] instead of thermally induced crystallization. This point will become clearer later when the crystallization of a 50/50 blend, which has an even sharper secondary peak, is discussed. The T_g of the 60% PVF_2 blend measured by a second DSC scan is 37°C [Fig. 4(C)] or about 12°C higher than room temperature. During ambient storage, this polymer is in an excellent condition to undergo sub-T_g annealing but not to experience thermally induced crystallization. Exposing this polymer to diluent environments, however, can depress its T_g, which in turn can induce crystallization. The effects of CO_2 sorption on secondary PVF_2 crystallization are shown in Figure 6, where DSC scans for samples which have been exposed to various CO_2 pressures and 25 atm N_2 are compared. The purpose of including N_2 in the comparison is to see if gases which are much less soluble are capable of inducing secondary crystallization. As may be seen by comparing scans A and B in Figure 6, N_2 has essentially no effect on crystallinity even up to a pressure of 25 atm since the DSC scans before

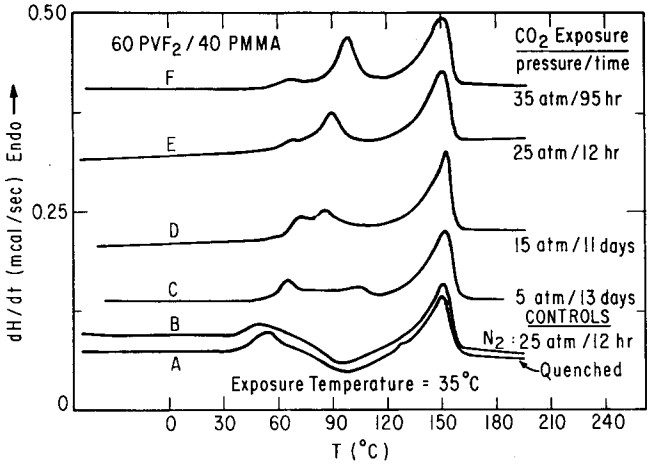

Fig. 6. First heat thermograms for 60% PVF_2 blends following gas exposure conditions shown. All gas exposure done at 35°C.

and after N_2 exposure are almost identical. The sorption of N_2 in the polymer is a factor of 28 by weight lower than that of CO_2,[11] and obviously this difference is quite significant in terms of the effect on the segmental motions of the polymer and, thus, on any propensity to facilitate crystallization. It can be assumed that other gases such as He, Ar, and Ch_4, which also have much lower gas solubility coefficients than CO_2, will have little ability to induce crystallization. On the contrary, gases with solubility coefficients comparable to CO_2, such as SO_2, NO_2, and NH_3, are expected to be active agents for inducing crystallization.

Figure 6 demonstrates very significant crystallization effects are observed when a 60% PVF_2 blend is exposed to CO_2. Even at exposure pressures as low as 5 atm, significant changes are seen. For example, scan C in Figure 6 reveals that crystallization on heating in the DSC, which shows up as an exothermic peak in scan A for the initial quenched sample, has disappeared after the CO_2 exposure indicated. Increasing the CO_2 pressure from 5 to 15 atm induces a small secondary peak just above the glass transition. This secondary peak shifts to higher temperatures and increases in magnitude as the CO_2 pressure is further elevated. At 35 atm of CO_2, the secondary peak has a magnitude comparable to the primary peak [Fig. 6(F)], and the boundary between them has become less distinguishable. It is interesting to note that CO_2 pressure or concentration has a similar effect as annealing temperature on the secondary PVF_2 melting endotherm. Increasing either variable causes the peak area to increase and to shift to higher temperatures. These responses may be interpreted as resulting from increased mass of these crystals and an increase in their individual sizes, respectively.

The parallels between crystallization induced by diluent sorption and by thermal annealing[20] are made clearer by the discussion which follows. Both approaches have the effect of enhancing the polymeric segmental motions so that molecular rearrangements needed for crystallization become kinetically possible. To compare these two approaches, thermally induced crystallization of the quenched 60% PVF_2 sample at 35, 70, and 97°C are

shown in Figure 7. Heating the sample to 35°C, which is still slightly lower than the T_g of the sample, does not induce discernible crystallization [Fig. 7(G)]. Elevating the temperature to 70°C, which is about 30°C above the T_g of the initial sample, effectively eliminates the original enthalpic relaxation peak and induces a secondary melting peak [Fig. 7(F)]. That the result in Figure 7(F) is nearly the same as that of Figure 6(F) indicates that thermal or sorption effects can lead to the same crystalline state if the conditions are appropriately matched. Further increasing the temperature to 97°C results in a secondary peak superposing on the shoulder of the primary one [Fig. 7(E)].

Since the extent of induced crystallization is not only a function of the thermal or sorption conditions but also of time, the results shown in this paper are not equilibrium ones. In other words, the magnitude and the apex temperature of the induced peak for a certain sorption pressure or certain temperature might be changed further if the time at this condition is prolonged. This is illustrated in Figures 7(A)–7(E) for thermally induced crystallization and in Figure 8 for sorption induced crystallization. The 60% PVF_2 blend when thermally annealed at 97°C undergoes crystallization as seen in Figure 7. The original exothermic peak disappears and a small endothermic peak appears within 10 min [Fig. 7(D)]. In addition, the apex temperature of the secondary peak and the glass transition temperature are also shifted to higher values. The T_g shift is the result of removal of PVF_2 from the amorphous phase to form crystals leaving a PMMA-enriched amorphous phase. In a similar fashion, the kinetic behavior for sorption induced crystallization is demonstrated in Figure 8, where a 50/50 blend is exposed to 25 atm of CO_2 for various times. The original extruded 50/50 sample shows a large enthalpic relaxation peak formed by sub-T_g annealing [Fig. 8(A)] because it has a T_g of 47°C, which is 22°C higher than room temperature. Interestingly, this peak is diminished by exposing the sample to 25 atm of CO_2 gas for 2 h [Fig. 8(B)]. Chan and Paul[21] have reported similar effects for polycarbonate. The T_g of this polymer plus sorbed CO_2

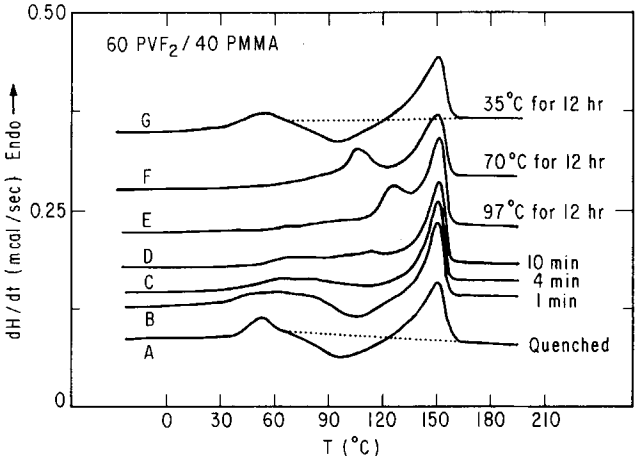

Fig. 7. Illustration of time effects on thermally induced secondary crystallization of PVF_2 from blends containing 60% PVF_2.

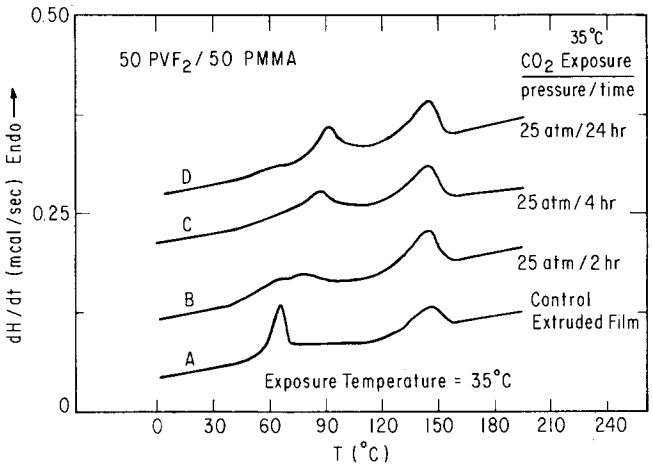

Fig. 8. Effect of CO_2 exposure time on 50% PVF_2 blends.

in the equilibrium amount at 25 atm is estimated to be 25°C,[10] which is below the sorption temperature, 35°C. Thus, CO_2 sorption has changed the polymer from being in the glassy state at 35°C to being in the rubbery state. Thus, CO_2 sorption in this case is, in effect, the same as heating the sample to a temperature higher than its T_g and CO_2 desorption is the same as cooling it to a temperature below T_g. Either protocol should eliminate the prior history of a glassy polymer. However, it should be noted that the sorption and the heating processes would cause opposite results if the DSC peak were a secondary melting endotherm instead of resulting from enthalpic relaxation. Heating the sample above its T_g and quenching should eliminate the DSC peak no matter whether it originated from melting or enthalpic relaxation. Depressing the T_g of the sample below the sorption temperature by dissolved CO_2, however, would eradicate an enthalpic relaxation peak but enhance an originally existing melting peak to an even larger one with a higher apex temperature. This difference allows us to distinguish a secondary peak caused by enthalpic relaxation from one caused by melting of small crystallites. The result of Figure 8(B) obviously confirms that the initial secondary peak is caused by enthalpic relaxation.

40% PVF_2 Blend

Quenched blends containing 40% PVF_2 are totally amorphous and have a T_g of 53°C [Fig. 9(A)]. By annealing at 35°C, an enthalpic relaxation peak [Fig. 9(B)] like those found for the 60% and 50% PVF_2 blends is formed. By exposing this blend to 10 atm of CO_2, which reduces the T_g to 37°C,[10] the relaxation peak is shifted up the temperature scale and it becomes an overshoot of the glass transition [Fig. 9(C)]. However, the 40% blend is relatively inactive with respect to crystallization induced by gas sorption. Even when exposed to CO_2 for 24 h at 20 and 30 atm [Fig. 9(D) and (E)] the crystallinities developed are only 3 and 5%, respectively, as compared to 16% for the 50% blend at 25 atm. While in the presence of CO_2 at 20 and 30 atm, the glass transitions are estimated[10] to be 32 and 20°C, respectively;

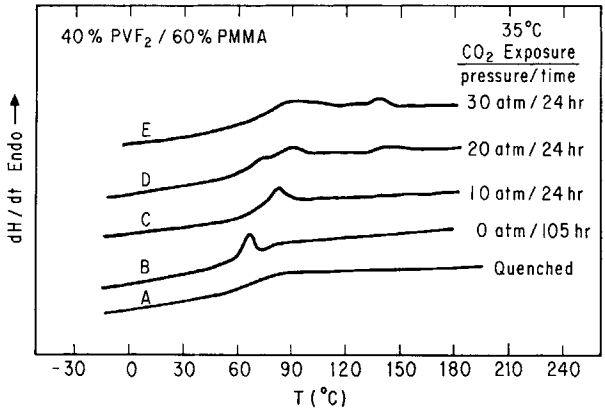

Fig. 9. Results for blend containing 40% PVF_2.

however, the large quantity of very viscous PMMA apparently decreases the rate of PVF_2 crystallization such that more crystallinity cannot be developed in the time allowed. Blends with lower PVF_2 concentrations, like the 20% PVF_2 mixture, have even more severe limitations on rate, and no induced crystallinity was observed. The humps seen in thermograms for the 20% blend [Figs. 2(E) and 3(E)] are due to sub-T_g enthalpic relaxation, not melting, since they occur below T_g.

Poly(ethylene Terephthalate)

The effects described above are not unique to PVF_2 blends, and, to demonstrate this generality, the study was extended. PET was chosen as another material to examine because of its commercial importance and the previous literature on its vapor- and solvent-induced crystallization. DSC scans for PET under various conditions are shown in Figure 10. Scan A is a first

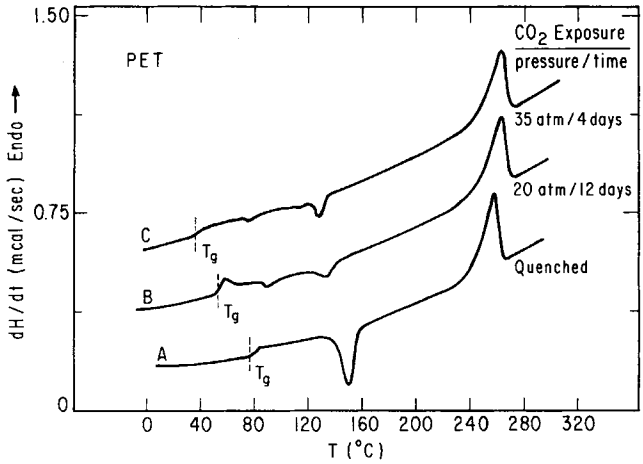

Fig. 10. Results for poly(ethylene terephthalate). Note that curves B and C were run attempting to retain sorbed CO_2 in the sample so that T_g's noted reflect plasticization by the dissolved CO_2.

heat for PET quenched from the melt. Prior to traversing the glass transition, T_g = 74°C, the quenched PET has rather low crystallinity as seen by the comparable size of the crystallization and melting peaks. Scans B and C were run after exposure to CO_2 for the conditions indicated without first removing the CO_2—as described earlier,[10] this technique provides an estimate of the T_g for the polymer–CO_2 mixture since desorption is not rapid relative to heating in the DSC. Based on these results, T_g is depressed to at least 52°C by CO_2 sorbed at 20 atm and to 35°C by CO_2 at 35 atm. Note that a heat capacity overshoot or endothermic peak occurs after T_g for Figure 10(B) but not for Figure 10(C). This suggests that, at 35°C, the sample exposed to 20 atm of CO_2 is still below T_g while that exposed to 35 atm is above T_g.

While the three endothermic melting peaks in Figure 10 have about the same ΔH_m of 11.0 cal/g, the magnitudes of the exothermic crystallization peaks for scans A, B, and C are -7.2, -2.5, and -1.4 cal/g, respectively. The as-received PET had a ΔH_m of 11.8 cal/g and a zero ΔH_c with crystallinity of 59±2% by density or 61±5% by X-ray measurement.[22] Thus, the crystallinity of the quenched PET was increased from the 19.3 to 43.1 and 48.7% during 20 and 35 atm CO_2 sorption, respectively. It should be noted that apparently crystallization of PET is induced at 20 atm of CO_2 in spite of the fact that its T_g is estimated, by the DSC technique, to be higher than the temperature at which crystallization is believed to occur. Obviously more work would be needed to understand fully this result.

The results in Figure 10 are similar to those reported by Lin and Koenig[4] for benzene-induced crystallization of PET. This confirms that a gas like CO_2 can be as effective as a solvent for inducing crystallization in some polymers.

Orientation Effects

By virtue of the nature of the extrusion process used to prepare the films employed in this study, a certain amount of molecular orientation existed in each sample. The extent of orientation as determined by birefringence measurements depends on the amount of drawdown employed, or the final film thickness, as illustrated for one set of samples in Figure 11. In this

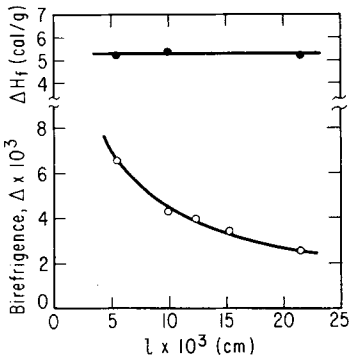

Fig. 11. Birefringence and PVF_2 heat of fusion for film containing 60% PVF_2 drawn down to different thicknesses during extrusion. Measurements were made after exposure to CO_2 at 25 atm for 26 h.

case, thinner films were made by increasing the drawdown; hence, birefringence is related to final thickness as shown. As shown by the ΔH_f data, the level of crystallinity is independent of film thickness. At a fixed drawdown, the extent of molecular orientation as indicated by birefringence is a strong function of blend composition as shown by curve B in Figure 12. Birefringence increases with PVF_2 content just as the level of crystallinity does (see Fig. 1). This suggests that crystalline orientation is a more important contributor to the birefringence shown by these samples than is amorphous orientation. However, the extent of birefringence depends on the extent of drawdown used in the extrusion process. Film prepared as part of this work[10-12] by solvent casting or by melting extruded film to relax it showed zero birefringence even for pure PVF_2 as expected.

Based on the observations that follow, it is apparent that the additional crystalline material formed by exposure to CO_2 has similar orientation to that in the original materials. Curve A in Figure 12 shows that the birefringence of these materials *increases* as a result of exposure to CO_2 at 25 atm for 25 h. Owing to the plasticizing effect CO_2 has on the amorphous phase, one might have expected a reduction in birefringence if amorphous orientation were a major factor. Using the data in Figures 1 and 12, the changes in birefringence and the heat of fusion for each blend caused by CO_2 exposure can be related as seen in Figure 12 where the notations "a" and "b" are used to denote *after* and *before* CO_2 exposure, respectively. The increase in birefringence is proportional to the increase in crystallinity, thus supporting the proposal that the crystalline material formed by CO_2 exposure is preferentially oriented in the extrusion direction of the film. The scatter in Figure 13 is primarily a result of thickness or drawdown variations among the various samples. The data points in Figures 12 and 13 are mostly based on film specimens having thicknesses of 4–5 mils. The range bars shown for several points in Figure 12 were drawn to illustrate this effect rather than experimental errors. However, it was not possible to account for this effect exactly in constructing Figure 13.

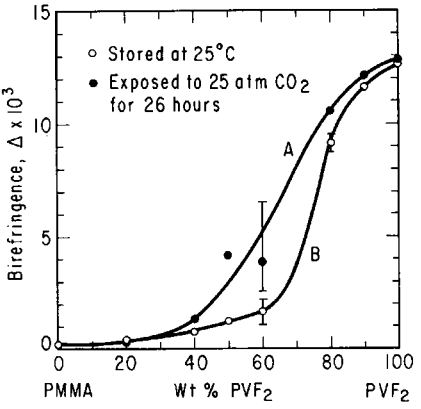

Fig. 12. Birefringence of extruded blend film stored at room temperature (B) (○) and after exposure to CO_2 at 25 atm for 26 h at 35°C (A) (●).

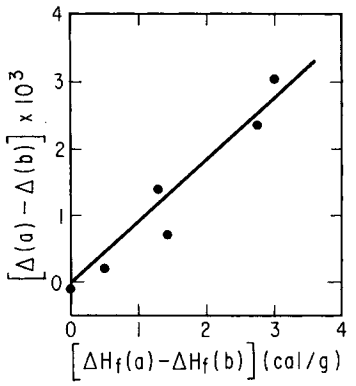

Fig. 13. Correlation of increase in birefringence with increase in heat of fusion after (a) exposure to CO_2 relative to samples before (b) this exposure. Data from Figures 1 and 12.

CONCLUSIONS

This study has shown that high pressure sorption of CO_2 gas can induce crystallization in certain polymers just as appropriate vapors or liquids can. Miscible blends of PVF_2 and PMMA provide a convenient system of materials for examining this phenomenon although selected experiments with poly(ethylene terephthalate) demonstrate generality. Other work has shown that CO_2 sorption can cause significant lowering of the glass transition temperature[10] just a sorption of liquids or vapors do. This plasticization can facilitate crystallization of polymers which are able to crystallize but have not done so to their usual extent and are kinetically restricted from doing so at the temperature of sorption.

The CO_2-induced crystallization in PVF_2/PMMA blends causes the appearance of a secondary melting endotherm varying in location from just above the T_g of the material to just below the normal PVF_2 melting point. In some cases, the peak appears similar in size and location to the familiar heat capacity overshoot, or enthalpic relaxation, associated with sub-T_g annealing; however, by appropriate methods peaks originating from these two causes could be distinguished. The secondary melting endotherm for PVF_2 also appears following appropriate thermal annealing. Its location and area are seen to change in systematic and physically reasonable ways as temperature, blend composition, CO_2 pressure, and time varied. This peak evidently arises from the melting of crystals formed under restricted conditions and are, thus, significantly smaller than normally formed from PVF_2 systems. Based on birefringence observations, the crystals formed in this secondary step tend to have the same preferential orientation, if any, which existed in the material originally. A similar finding has been reported[23] for vapor-induced crystallization of *s*-PMMA stretched in the amorphous state.

This research was supported by the U.S. Army Research Office.

References

1. W. R. Moore and R. P. Sheldon, *Polymer*, **2**, 315 (1961).
2. A. B. Desai and G. L. Wilkes, *J. Polym. Sci., Polym. Symp.*, **46**, 291 (1974).

3. H. Jameel, J. Waldman, and L. Rebenfeld, *J. Appl. Polym. Sci.*, **26**, 1795 (1981).
4. S. B. Lin and J. L. Koenig, *J. Polym. Sci., Polym. Phys. Ed.*, **21**, 1539 (1983).
5. R. P. Kambour, F. E. Karasz, and J. H. Danne, *J. Polym. Sci., A-2*, **4**, 327 (1966).
6. E. Turka and W. Benechi, *J. Appl. Polym. Sci.*, **23**, 3489 (1979).
7. R. A. Ware, S. Tirtowidjojo, and C. Cohen, *J. Appl. Polym. Sci.*, **26**, 2975 (1981).
8. R. A. Assink, *J. Polym. Sci., Polym. Phys. Ed.*, **12**, 2281 (1974).
9. W. V. Wang, E. J. Kramer, and W. H. Sachse, *J. Polym. Sci., Polym. Phys. Ed.*, **20**, 1371 (1982).
10. J. S. Chiou, J. W. Barlow, and D. R. Paul, **30**, 2633 (1985).
11. J. S. Chiou, Ph.D. dissertation, University of Texas at Austin, 1985.
12. J. S. Chiou, J. W. Barlow, and D. R. Paul, to appear.
13. D. R. Paul, J. W. Barlow, R. E. Bernstein, and D. C. Wahrmund, *Polym. Eng. Sci.*, **13**, 1225 (1978).
14. D. R. Paul and J. W. Barlow, *Polym. Sci. Technol.*, **11**, 239 (1979).
15. R. S. Morra and R. S. Stein, *J. Polym. Sci., Polym. Phys. Ed.*, **21**, 2243 (1982).
16. R. F. Boyer, *J. Polym. Sci.*, **50C**, 189 (1975).
17. S. E. B. Petrie, *J. Polym. Sci., A-2*, **10**, 1255 (1972).
18. I. M. Hodge and A. R. Berens, *Macromolecules*, **15**, 756 (1982).
19. I. M. Hodge and G. S. Huvard, *Macromolecules*, **16**, 371 (1983).
20. A. S. Ribnick, H. D. Weigmann, and L. Rebenfield, *Text. Res. J.*, **42**, 720 (1972).
21. A. H. Chan and D. R. Paul, *J. Appl. Polym. Sci.*, **24**, 1539 (1979).
22. W. J. Koros, Ph.D. dissertation, University of Texas at Austin, 1977.
23. H. Kusuyama, M. Takase, Y. Higashihata, H. T. Tseng, Y. Chatani, and H. Tadokaro, *Polymer*, **23**, 1256 (1982).

Received October 10, 1984
Accepted January 9, 1985